



Experimental Research Article

Korean J Anesthesiol 2023;76(3):252-260

<https://doi.org/10.4097/kja.22499>

pISSN 2005-6419 • eISSN 2005-7563

Received: August 9, 2022

Revised: September 25, 2022

Accepted: October 6, 2022

Corresponding author:

Hun-Mu Yang, Ph.D.

Department of Anatomy, Yonsei University

College of Medicine, 50 Yonsei-ro,

Seodaemun-gu, Seoul 03722, Korea

Tel: +82-2-2228-1649

Fax: +82-2-365-0700

Email: yanghm@yuhs.ac

ORCID: <https://orcid.org/0000-0003-1954-0114>

*Shin Hyo Lee and Hee Jung Kim are contributed equally to this work as first authors.

†Shin Hyo Lee is now with the Department of Anatomy and Jesaeng-Euise Clinical Anatomy Center, Wonkwang University School of Medicine, Iksan, Korea

‡Tae-Hyeon Cho is now with the Department of Anatomy, College of Korean Medicine, Semyung University, Jecheon, Korea



© The Korean Society of Anesthesiologists, 2023

© This is an open-access article distributed under the terms of the Creative Commons Attribution Non-Commercial License (<http://creativecommons.org/licenses/by-nc/4.0/>) which permits unrestricted non-commercial use, distribution, and reproduction in any medium, provided the original work is properly cited.

Anatomical study of the adductor canal: three-dimensional micro-computed tomography, histological, and immunofluorescence findings relevant to neural blockade

Shin Hyo Lee^{1,2,*†}, Hee Jung Kim^{2,3,*}, Shin Hyung Kim^{2,3},
Tae-Hyeon Cho^{1,2,‡}, Hyun-Jin Kwon^{1,2}, Jehoon O⁴, Ju Eun Hong⁵,
Seung Hyun Nam³, Young-Il Hwang⁶, Hun-Mu Yang^{1,2,7}

¹Department of Anatomy, Yonsei University College of Medicine, ²Translational Research Unit for Anatomy and Analgesia, ³Department of Anesthesiology and Pain Medicine, Yonsei University College of Medicine, ⁴Center of Biohealth Convergence and Open Sharing System, Hongik University, Seoul, ⁵Department of Biomedical Laboratory Science, College of Software and Digital Healthcare Convergence, Yonsei University MIRAE Campus, Wonju, ⁶Department of Anatomy and Cell Biology, Seoul National University College of Medicine, ⁷Surgical Anatomy Education Center, Yonsei University College of Medicine, Seoul, Korea

Background: A precise anatomical understanding of the adductor canal (AC) and its neural components is essential for discerning the action mechanism of the AC block. We therefore aimed to clarify the detailed anatomy of the AC using micro-computed tomography (micro-CT), histological evaluation, and immunofluorescence (IF) assays.

Methods: Gross dissections of 39 thighs provided morphometric data relevant to injection landmarks. Serial sectional images of the AC were defined using micro-CT and ultrasonography. The fascial and neural structures of the AC proper were histologically evaluated using Masson's trichrome and Verhoeff-Van Gieson staining, and double IF staining using choline acetyltransferase (ChAT) and neurofilament 200 antibodies.

Results: The posteromedial branch insertion of the nerve to vastus medialis (NVM) into the lateral border of the AC proper was lower (14.5 ± 2.4 cm [mean \pm SD] above the base of the patella) than the origin of the proximal AC. The AC consists of a thin subsartorial fascia in the proximal region and a thick aponeurosis-like vastoadductor membrane in the distal region. In the proximal AC, the posteromedial branch of the NVM (pmNVM) consistently contained both sensory and motor fibers, and more ChAT-positive fibers were observed than in the saphenous nerve ($27.5 \pm 11.2 / 10^4$ vs. $4.2 \pm 2.6 / 10^4$ [counts/ μm^2], $P < 0.001$).

Conclusions: Anatomical differences in fascial structures between the proximal and distal AC and a mixed neural component of the neighboring pmNVM have been visualized using micro-CT images, histological evaluation, and IF assays.

Keywords: Anatomy; Anesthesia; Cadaver; Fascia; Histology; Immunohistochemistry.

Introduction

The adductor canal (AC) is an intermuscular tunnel that conveys the saphenous nerve (SN) bordered by the vastus medialis (VM), adductors, and sartorius muscles [1]. The AC surface is covered by a musculotendinous band called the vastoadductor membrane

(VAM) on the distal progression of the AC roof, which is a strong fascia that extends between the fasciae investing the border muscles [2,3]. The physiological extension of the interfascial space and the composition of the fascial roof of the AC are important factors affecting the spread of the injectate to the SN that innervates the knee joint [4,5]. Not much is known about the entire fascial AC structures, although previous clinical trials have attempted to evaluate the differences in the analgesic efficacy of AC blocks according to their target locations [6-9]. Furthermore, the axonal components of the posteromedial branches of the nerve to the vastus medialis (pmNVM) that travel along the SN have been predicted by their innervation patterns from gross observations, but not based on the histological evidence [10-12].

We therefore aimed to comprehensively determine the regional structural features of the AC and pmNVM using three-dimensional micro-computed tomography (3D micro-CT), macroscopic and histological inspections, and ultrasonography. We also investigated the motor and sensory axonal components of the SN and pmNVM at the AC level using immunofluorescence (IF) assays.

Materials and Methods

Study oversight

We obtained appropriate consent to use cadavers that had been legally donated to the Surgical Anatomy Education Center of the Yonsei University College of Medicine (Approval no. 22-001). Before they died, each donor signed documents agreeing to their participation in the body donation program of the medical school and to the use of their body for clinical studies. The study design was approved by the Institutional Review Board of Yonsei University Health System, although the board exempted this study from a formal review due to its use of cadavers. This study was conducted in accordance with the Declaration of Helsinki (2013).

Sample recruitment

This study used 29 cadavers (14 male and 15 female) with a mean age at death of 82.2 years. Specimens with visible signs of deformity and previous operative procedures in the thigh were excluded. Gross dissections and conventional macroscopic examinations were performed on 39 thighs from 21 embalmed cadavers to analyze the morphometry of the structures relevant to the AC. A 3D topographic analysis of the micro-CT images and histological revalidation were performed on four embalmed cadavers. Ultrasonographic images were obtained from one fresh ca-

daver. Within 48 h of death, three fresh non-embalmed refrigerated cadavers were investigated using double IF assays on their nerves within the AC.

Morphometry of the AC and relevant structures

Experienced anatomists dissected the entire thighs including their inguinal region, femoral triangle (FT), AC, adductor hiatus (AH), and base of the patella (PB). All distances from the PB to anatomical landmarks were measured using a ruler: (1) anterior superior iliac spine, (2) apex of the FT, (3) insertion of the pmNVM into the VM fascia, (4) proximal VAM border, (5) exit point of the SN from the AC, and (6) proximal end of the AH. In this study, the proximal AC was defined as the proximal part of the AC, which is covered by the thin subsartorial fascia roof and reaches from the apex of the FT to the proximal border of the thick VAM.

Micro-CT preparation for 3D visualization

Based on the thigh morphometry results, four anteromedial thigh specimens from four embalmed cadavers were transected in the axial plane at 6-cm intervals. The musculofascial tissue blocks that preserve the neurovascular contents of each specimen were dehydrated with a graded series of 30%, 50%, and 70% ethanol solutions for one night each, and then soaked with phosphotungstic acid to enhance the soft-tissue contrast through active infiltration of treatment solutions without losing the relevant AC landmarks described in Fig. 1. Micro-CT images were acquired using a micro-CT scanner (Skyscan 1173, Bruker, Belgium) with a 70-kV source voltage, 114- μ A source current, and 35- μ m² images. For 3D visualization and analysis, the acquired sectional images were reconstructed using NRecon and CTVOX (Bruker). The 3D images representative of the AC are provided in [Supplementary Video 1](#).

AC histomorphology and neural components analysis

Tissue block specimens used for micro-CT analysis then underwent routine histological processing and cut into 5- μ m-thick sections, which were stained using Masson's trichrome and Verhoeff-Van Gieson to compare the fascial components of the proximal and distal parts of the AC. Choline acetyltransferase (ChAT) selectively labels peripheral motor axons in humans [13]. To quantify motor and sensory makeup of the pmNVM and SN, sections were incubated with the primary antibody against neurofilament 200 (NF200; mouse, diluted 1:400; Abcam) and ChAT (goat,

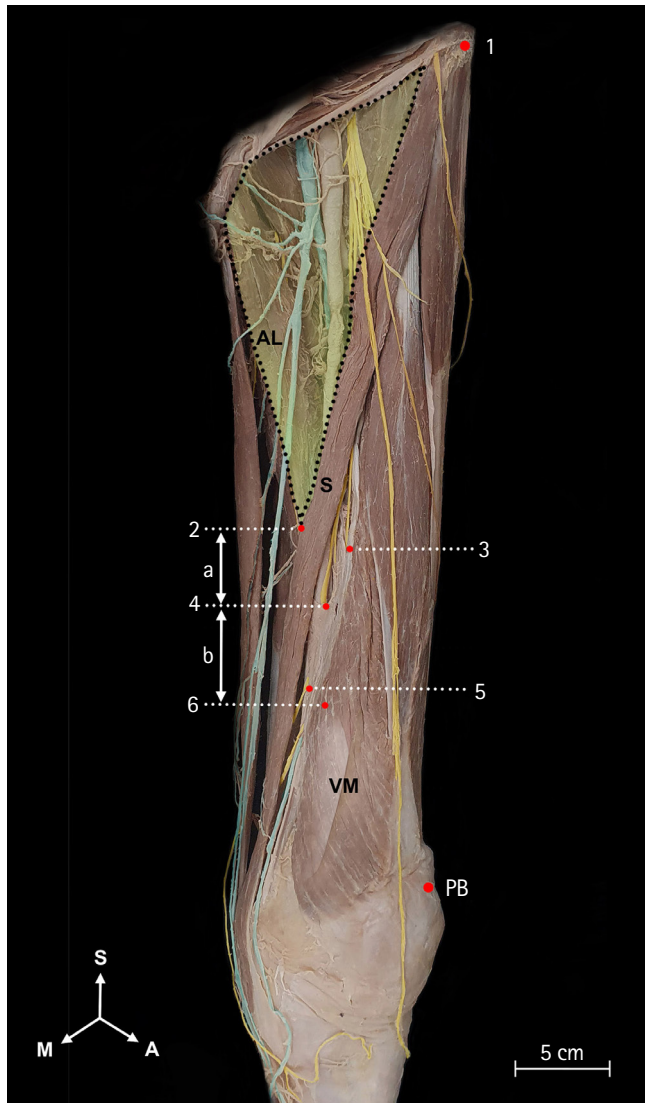


Fig. 1. Morphometry of the AC-related structures. Measured distances are listed in Table 1. AC: adductor canal, AH: adductor hiatus, AL: adductor longus, FT: femoral triangle, PB: base of patella, pmNVM: posteromedial branch of the nerve to vastus medialis, S: sartorius, SN: saphenous nerve, VAM: vastoadductor membrane, VM: vastus medialis, green area: FT, 1: anterior superior iliac spine, 2: FT apex, 3: entry point of the pmNVM, 4: proximal margin of the VAM, 5: exit site of the SN from AC, 6: proximal end of the AH, a: proximal AC, b: distal AC.

diluted 1:100; Abcam). Antigens were observed in each section using the Abcam Alexa Fluor 488 donkey antimouse IgG and Abcam Alexa Fluor 555 donkey antigoat IgG. The ratio of ChAT-positive neurons to the cross-sectional area of each fascicle was computed in microns squared for each cross-sectional image (Image J version 1.53n, NIH, USA).

Table 1. Morphometric Data of Structures Relevant to the VAM

Measure	Value
1. PB to ASIS	41.3 ± 1.5
2. PB to FT	19.0 ± 1.5
3. PB to X	14.5 ± 2.4
4. PB to Y	13.7 ± 1.8
5. PB to Z	10.6 ± 2.4
6. PB to AH	9.4 ± 1.8
a. Proximal AC	5.2 ± 2.0
b. Distal AC	4.3 ± 1.5

Values are mean ± SD values in centimeters. AC: adductor canal (entire AC = a + b), AH: adductor hiatus, ASIS: anterior superior iliac spine, FT: femoral triangle apex, PB: base of patella, pmNVM: posteromedial branch of the nerve to vastus medialis, SN: saphenous nerve, VAM: vastoadductor membrane, VM: vastus medialis, X: insertion of the pmNVM to the lateral border of the AC proper, Y: proximal margin of the VAM originating from the VM, Z: exit site of the SN from the AC.

Statistical analysis

Morphometric data are presented as mean ± SD values. To compare motor axon counts between the pmNVM and SN at the proximal AC, the nonparametric Mann–Whitney *U* test was used due to the non-normal data distribution. All statistical analyses were performed using the Statistical Package for the Social Sciences (version 25.0, IBM Corp., USA), and $P < 0.05$ was considered significant.

Results

AC topography

The AC is a subsartorial fascial compartment anterolaterally bordered by the VM and posteromedially by the adductor longus (AL) or adductor magnus (AM) muscles. Measurements from 39 thighs were used to determine the distances between the PB and relevant landmarks (Fig. 1, Table 1). The AC was subdivided into its proximal and distal parts according to the fascia thickness. The apex of the FT (intersection of the medial borders of the sartorius and AL muscles) was considered as the beginning of the proximal AC. The beginning of the proximal AC (19.0 ± 1.5 cm from the PB) was approximately 2 cm more distal than the midpoint of the thigh (21 cm from the PB). The proximal AC roof was covered with thin fascia. At 13.7 ± 1.8 cm from the PB, the fascia became distinctly thickened (the true VAM) in all specimens. The length of the entire AC between the apex of the FT and the AH was approximately 9.5 cm. The mean length of the proximal AC invested by the thin subsartorial fascia was 5.2 cm,

and the mean length of the distal AC invested by the thick VAM was 4.3 cm. The entry point of the pmNVM into the lateral VM border was within the proximal AC (14.5 ± 2.4 cm from the PB) in 38 of 39 specimens. In one specimen the entry point was proximal to the apex of the FT.

AC structures by micro-CT images and ultrasound imaging

The micro-CT images allowed observation of the intact structures of the AC contents without deformation due to performing direct dissection. In the proximal AC, a thin superficial layer of

the subsartorial fascia traversing between the AL and VM was close to the femoral artery. More distally, the thick VAM appeared between the AM and VM in all specimens. With the change of the distal AC roof thickness, the transition of the AL/AM proportion (cross sectional area) in the medial boundary of the AC also coincided with the ultrasonography finding that the AM occupied more areas than the proximal AC (Fig. 2).

Both the comparative location of the nerves and the compartmentation of the fascial layers could be identified clearly on the micro-CT images. The subsartorial proximal AC fascia was connected to the fascial septum elongation from the fascia lata. Consecutively, a thick VAM originating from the VM fascia traversed

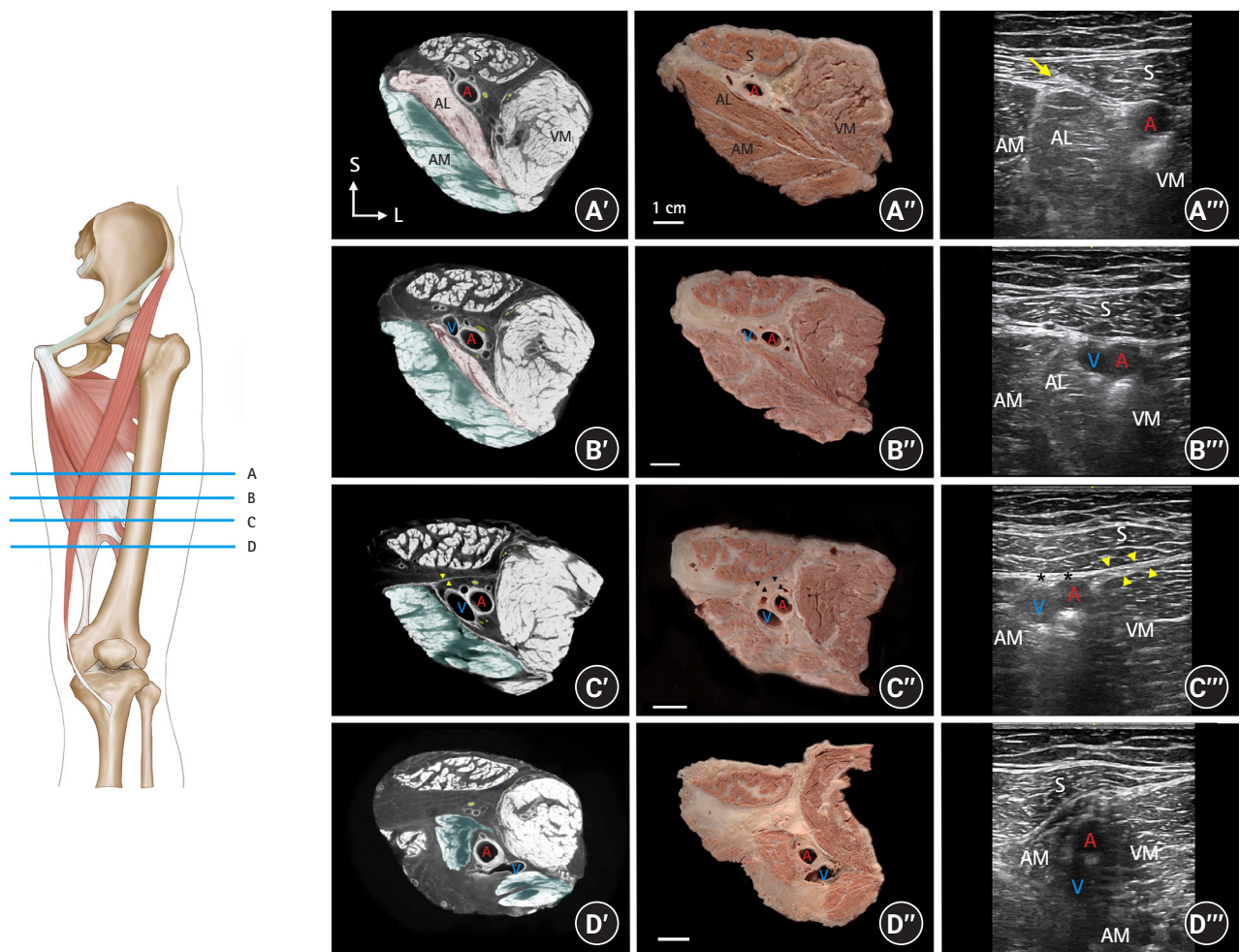


Fig. 2. Comparison of micro-CT, gross-section, and ultrasonography images according to the relative locations. The AC roof is positioned in a superficial position corresponding to the ultrasonographic positions. A'-D': Cross-sectional image of anteromedial thighs on micro-CT. The medial AC border consists of the AL (area shaded in pink) or AM (area shaded in green). Arrowheads indicate the VAM investing the distal AC. A''-D'': Gross sections of the same specimen. Arrowheads indicate the VAM. A''': Ultrasonography corresponding to the micro-CT and gross section images. The intersection of the sartorius and AL (arrow) indicates the apex of the FT, which is the initiation of the proximal AC. B''': The area of the AL decreased in the distal part of the proximal AC. C''': The thick VAM (asterisks) above the femoral vessels and the double contour of fascial layers of the VM and VAM (arrowheads) in the distal AC. D''': Descending femoral vessels divided the AM into the tendinous part (superficial) and femur insertion (deep) in the AH. A: femoral artery, AC: adductor canal, AL: adductor longus, AM: adductor magnus, FT: femoral triangle, micro-CT: micro-computed tomography, V: femoral vein, VAM: vastoadductor membrane, VM: vastus medialis.

toward the distal part of the AM, as the cross-sectional areas of the AL decreased toward the distal femur. Furthermore, the thin superficial fascia continued to the subsartorial proximal AC fascia invested between the subsartorial space and the distal AC VAM. This subsartorial fascia still existed continuously between the VM and semimembranosus muscles at the level below the AH (Fig. 3, Supplementary Video 1).

Configuration of the AC contents by histological observation

The fascia forming the AC roof, composed of the proximal thin and distal thick fascia, also differed with the anatomical site on microscopic analysis. In the proximal AC, a thin layer elongating from the fascia investing the FT, consisting of the subsartorial fas-

cia between the AL and VM, was connected to the femoral artery by loose connective tissues. At this level, the SN (the terminal femoral nerve branch) descended lateral to the femoral artery and medial to the VM. The pmNVM coursed adjacent to the SN and was encased by a thin fascia between the VM and subsartorial fascia at the proximal AC level (Fig. 4A). Contrary to the proximal AC, the pmNVM exited the subsartorial space and was separated from the SN in the AC proper at the distal AC level. The distal AC roof was identified as a double-layered structure with the appearance of an additional thick fascia in the deeper layer. The thin subsartorial fascia, which elongated from the FT invested the VAM as a superficial layer in the distal AC. Consequently, the distal AC roof was composed of multiple fascial layers. Microscopically, the VAM consisted of relatively parallel collagen bundles, compared to the subsartorial fascia that had thin collagen fibers

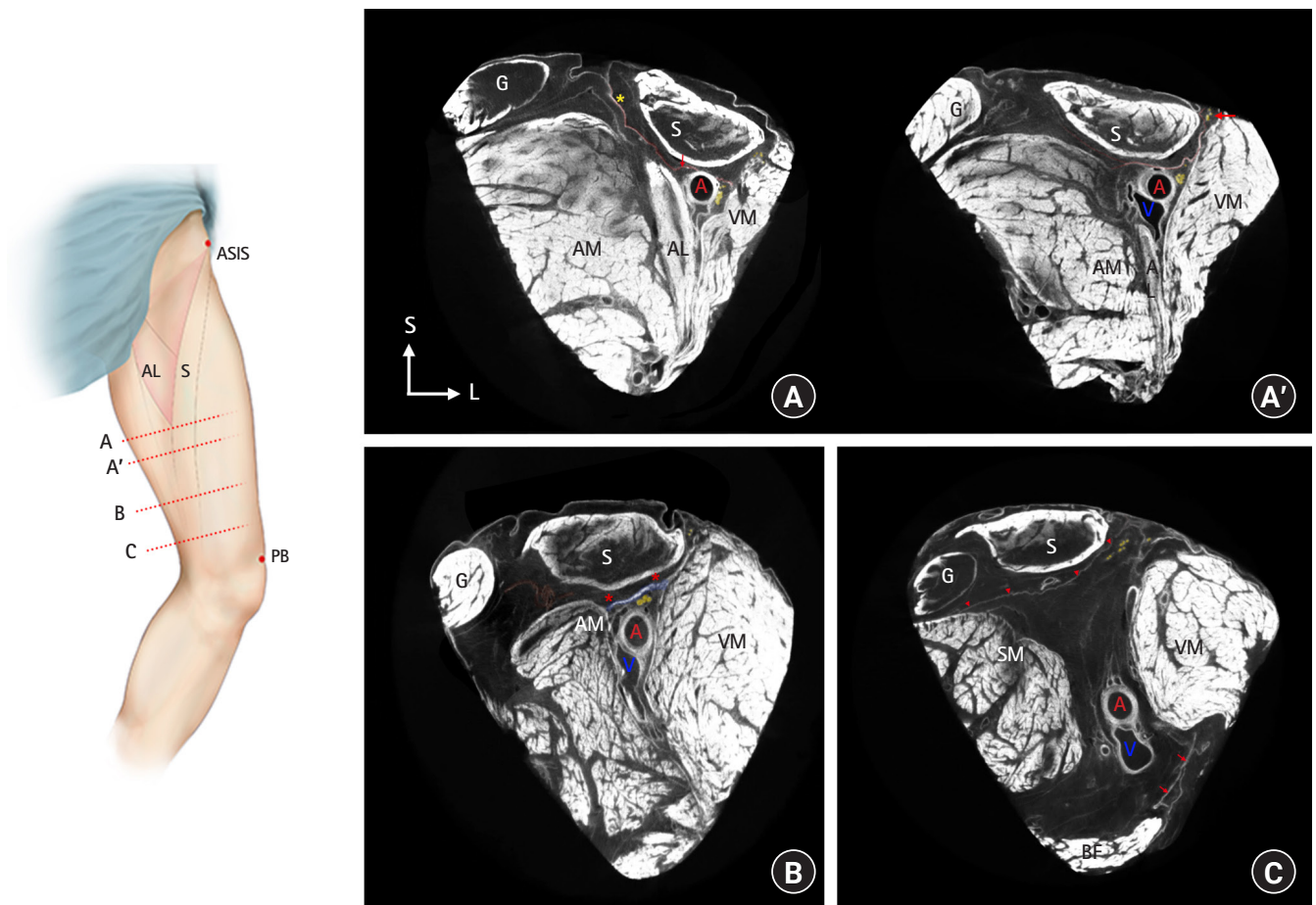


Fig. 3. Detailed micro-CT images of the AC. A: The appearance of the continuum of the fascia lata (asterisk) and subsartorial fascia (shaded in red). The SN (shaded in yellow) and the pmNVM (red arrow) are separated in the more distal section of the image (A'). B: The thick VAM (shaded in blue) inserted to the AM fascia. C: The subsartorial fascia (arrowheads) between the fascia lata and the semimembranosus muscle fascia and the posterior fascia (arrows) between the biceps femoris and the VM. AC: adductor canal, AM: adductor magnus, ASIS: anterior superior iliac spine, G: gracilis, micro-CT: micro-computed tomography, pmNVM: posteromedial branch of the nerve to vastus medialis, S: sartorius, SN: saphenous nerve, VAM: vastoadductor membrane, VM: vastus medialis.

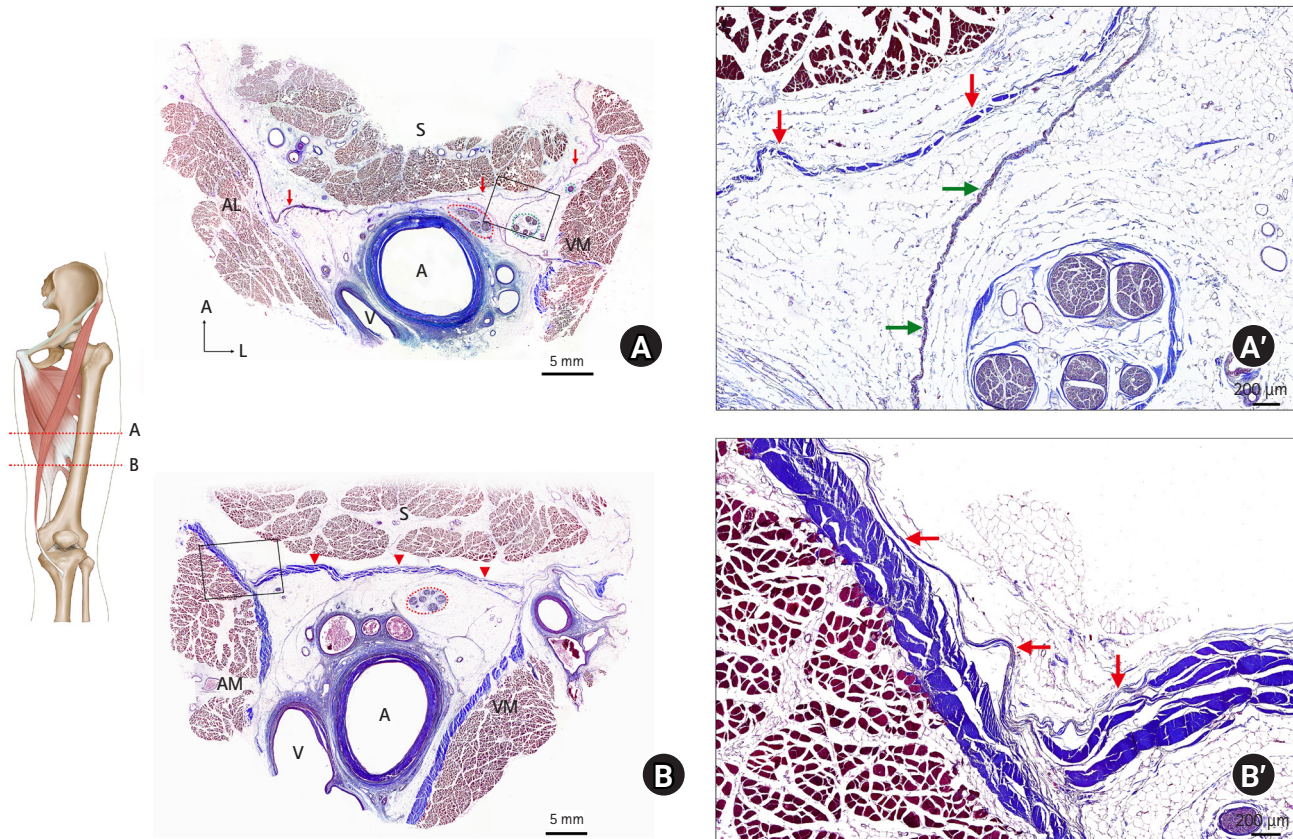


Fig. 4. Histology of the fascia investing the AC. A: A single layer of subsartorial fascia (arrows) at the apex of the FT level, the beginning of the proximal AC. Structures encircled by red and green dotted lines indicate the SN and pmNVM, respectively. A' : Magnification of the box in A. B: Distinct aponeurosis-like fascia (arrowheads) elongating from the VM fascia forming the barrier to the subsartorial space, as a distal AC roof. B' : Multiple VAM layers covered with superficial thin fascia (arrows) in a magnification of the box in B. AC: adductor canal, FT: femoral triangle, pmNVM: posteromedial branch of the nerve to vastus medialis, SN: saphenous nerve, VAM: vastoadductor membrane, VM: vastus medialis.

running in multiple directions with profound elastic fibers (Fig. 4B, Supplementary Fig. 1).

Axonal components analysis

The axonal components of the nerves related to the selective sensory block were identified by applying IF labeling to the transverse sections of the pmNVM and SN. Motor axon marker expression (ChAT) was dominantly identified in the pmNVM. In contrast, the SN mostly comprised ChAT-negative axons, with smaller diameters than the ChAT-positive motor axons in the pmNVM (Fig. 5). The double-positive axons counts (ChAT and NF200) per fascicle area confirmed that the proportion of motor axon population in the pmNVM was significantly greater than that in the SN at the proximal AC level ($27.5 \pm 11.2 / 10^4$ vs. $4.2 \pm 2.6 / 10^4$ [counts/ μm^2], $P < 0.001$). At low magnification, nerve fascicles that mostly comprised ChAT-negative axons were also identified in the pmNVM. This indicates that the pmNVM

in the proximal AC has a greater proportion of motor axons than the SN, and also a coexistence of motor- and sensory-dominant fascicles.

Discussion

This study used micro-CT and histological evaluation to confirm that the entire AC, from the apex of the FT to the AH, is roofed by multiple fascial layers, consisting of the proximal thin and distal thick parts of the AC. Our ultrasonography anatomical findings indicated that the starting point of the AC was the intersection of the medial borders of the sartorius and the AL, and identified the aponeurotic thick VAM as the AL became smaller. The pmNVM, separated from the AC proper by a thin fascia, contained a mixed axonal component with both motor and sensory fibers at the proximal AC level.

Recent anatomical studies have constantly observed a strong aponeurotic membrane in the distal part of the AC [1–3].

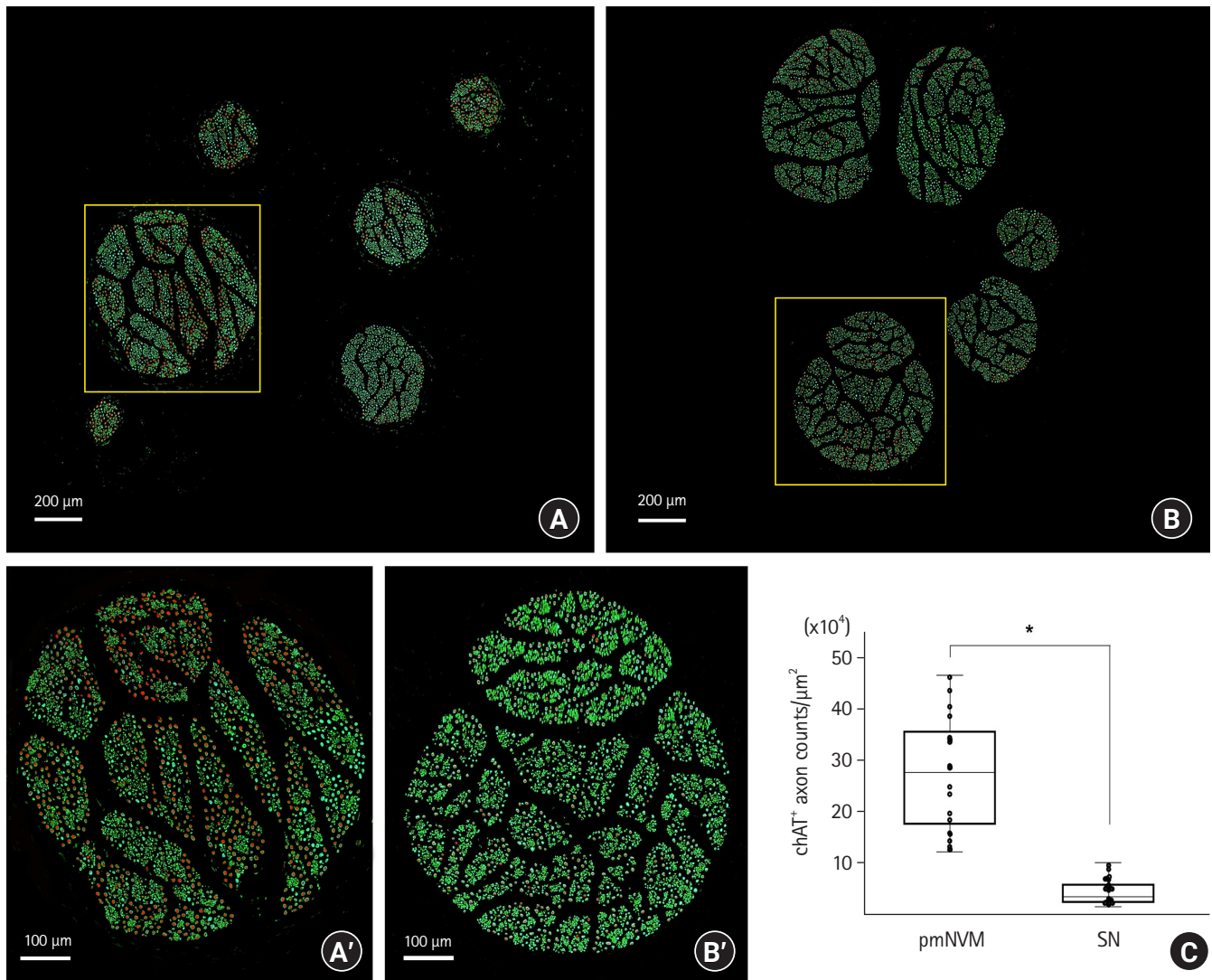


Fig. 5. Double IF staining using ChAT and NF200 antibodies to identify the axon components of the nerve fascicle. Low magnification images of the pmNVM (A) and SN (B) fascicles. A': Representative images of ChAT-positive axons in a pmNVM fascicle (magnification of the box in A). Red areas indicate motor nerve fibers overlapped by ChAT and NF200 signals. B': Magnification of the box in B. ChAT-negative axons (green) mostly consist of the SN in the proximal AC. C: Axon counts of double-positive ChAT and NF200 stains according to the area of each pmNVM and SN fascicle ($10^4 \mu\text{m}^2$). *: $P < 0.001$. AC: adductor canal, ChAT: choline acetyltransferase, IF: immunofluorescence, NF200: neurofilament 200, pmNVM: posteromedial branch of the nerve to vastus medialis, SN: saphenous nerve.

Bendtsen et al. [9] defined the fascial roof as the VAM and stated that the VAM divided the intramuscular space between the AC into the AC proper and the subsartorial space. Accordingly, our macroscopic findings confirmed that a distinct aponeurotic membrane, the VAM, presented only in the distal half of the AC. Moreover, ultrasonography findings from Wong et al. [14] indicated the VAM characteristic of a double contour at the distal AC. In our micro-CT image wherein the distal thick fascia overlapped the VM fascia, the AL occupied a very narrow area of the medial AC border. This suggests that ultrasonography can be used to identify the distal thick fascia, which begins at the level where the

section of the AL is almost absent.

This study found that a thin subsartorial fascia investing the proximal AC extended to the distal AC, as observed on the anterior side at the level below the AH using micro-CT images and histological assays. The subsartorial fascia of the FT traversing the proximal AC continuously invested the VAM in the distal AC. This result was consistent with Tran et al. finding that the distal AC was roofed by two superficial thin membrane layers and a deep aponeurosis of the VM obliquus (the lowest horizontal VM fibers) [11]. The subsartorial fascia, which elongates from the AC proper and continues to the superior region of the knee might re-

strict direct injectate spreading from the AC proper to the anterior knee. Instead, it would increase the risk of posterior leakage to the popliteal fossa after a distal AC block [14].

The distal pmNVM innervates most of the medial joint capsule [12,15], whereas the SN primarily provides cutaneous innervation. Based on studies of the gross anatomical branching patterns and the intramuscular passage of the nerve, the NVM has lateral proximal muscular branches running toward the superior part of the VM after coursing a short distance from the inguinal ligament, before terminating at the pmNVM descending along the SN [16]. An enhanced understanding of the entry point of the NVM branches may help refine the AC block approach and minimize quadriceps femoris weakness [17]. The most-inferior insertion of the pmNVM to the AC proper was mostly within the midpoint of the entire AC in the present study. The pmNVM laterally descends within its own fascia, separated from the AC proper in the proximal AC, whereas the pmNVM gradually exits the subarticular space of the distal AC proper (Fig. 4). This result supports the study of Tran et al. [11] finding that a dye injected into the proximal AC proper penetrates through the proximal thin roof and stains the pmNVM in cadavers. Moreover, we verified that the pmNVM is a mixed nerve and consists of both motor (ChAT-positive/NF200-positive) and sensory (ChAT-negative/NF200-positive) fibers. This is consistent with recent evidence that the pmNVM might also provide sensory innervation to the knee giving off the superior medial genicular nerve [12]. This result also implies that pmNVM blockade may lead to a certain amount of motor block. Further studies combined with the histological and morphometric methods could help clinicians refine the AC block technique.

This study had some limitations. The absolute axon counts of the motor and sensory proportions and the proximal courses of the NVM and SN with variant bifurcation patterns were not performed. The NVM and SN arose from the common femoral nerve branch in the proximal FT and then had the muscular branches lateral to the superior part of the VM [17]. This study intensively investigated the proximal AC region, and further studies are needed to clarify the anatomy and neural components of the distal AC and popliteal fossa region with larger sample sizes.

In conclusion, 3D micro-CT and histological investigations have revealed that the pmNVM, which is separated from the AC proper by a very thin fascia contains both sensory fibers and some motor fibers at the proximal AC level. Multidirectional observations using micro-CT, histology, and ultrasonography could assist clinicians in further investigating and refining neural blockade efficacy.

Acknowledgements

We are grateful to the people who very nobly donated their bodies to the Surgical Anatomy Education Centre at the Yonsei University College of Medicine. Additionally, the authors wish to thank Jun Ho Kim, Jong Ho Bang, and Tae-Jun Ha for their technical support (all are staff members of the Surgical Anatomy Education Centre at the Yonsei University College of Medicine).

Funding

This work was supported by the National Research Foundation of Korea (NRF) grant funded by the Korea government (No. 2020R1F1A1058123 to H-MY) and Basic Science Research Program through the NRF funded by the Ministry of Education (No. 2021R1F1A1045873 to SHK). No other external funding or competing interests declared.

Conflicts of Interest

No potential conflict of interest relevant to this article was reported.

Data Availability

All data generated or analyzed during this study are included in this published article and its supplementary information files.

Author Contributions

Shin Hyo Lee (Conceptualization; Formal analysis; Visualization; Writing – original draft)

Hee Jung Kim (Formal analysis; Methodology; Writing – original draft)

Shin Hyung Kim (Funding acquisition; Project administration; Supervision; Writing – review & editing)

Tae-Hyeon Cho (Data curation; Formal analysis; Software; Visualization)

Hyun-Jin Kwon (Data curation; Formal analysis; Investigation)

Jehoon O (Data curation; Methodology; Visualization)

Ju Eun Hong (Investigation; Methodology)

Seung Hyun Nam (Data curation; Methodology; Software)

Young-Il Hwang (Supervision; Writing – review & editing)

Hun-Mu Yang (Funding acquisition; Project administration; Resources; Supervision; Writing – review & editing)

Supplementary Materials

Supplementary Video 1. The 3D sectional micro-CT image correspondent to Fig. 3. A: femoral artery, AL: adductor longus, AM: adductor magnus, G: gracilis, pmNVM: posteromedial branch of the nerve to vastus medialis, S: sartorius, SM: semimembranosus, SN: saphenous nerve, V: femoral vein, VM: vastus medialis.

Supplementary Fig. 1. Verhoeff-Van Gieson staining of the AC. (A) Elastic fibers (black fragmented fibers) in the thin subsartorial fascia of the proximal AC. (B) Thick collagen bundles of the VAM. The magnification of the blue boxes. Blue dotted lines: SN, green dotted lines: pmNVM. A: femoral artery, AC: adductor canal, AM: adductor magnus, pmNVM: posteromedial branch of the nerve to vastus medialis, SN: saphenous nerve, V: femoral vein, VAM: vastoadductor membrane, VM: vastus medialis.

ORCID

Shin Hyo Lee, <https://orcid.org/0000-0001-7031-7722>

Hee Jung Kim, <https://orcid.org/0000-0002-2143-3943>

Shin Hyung Kim, <https://orcid.org/0000-0003-4058-7697>

Tae-Hyeon Cho, <https://orcid.org/0000-0001-7230-620X>

Hyun-Jin Kwon, <https://orcid.org/0000-0001-7752-6172>

Jehoon O, <https://orcid.org/0000-0003-4351-3183>

Ju Eun Hong, <https://orcid.org/0000-0002-5357-4476>

Seung Hyun Nam, <https://orcid.org/0000-0002-5736-2606>

Young-Il Hwang, <https://orcid.org/0000-0002-5777-7983>

Hun-Mu Yang, <https://orcid.org/0000-0003-1954-0114>

References

1. Uhl JE, Gillot C. Anatomy of the Hunter's canal and its role in the venous outlet syndrome of the lower limb. *Phlebology* 2015; 30: 604-11.
2. Tubbs RS, Loukas M, Shoja MM, Apaydin N, Oakes WJ, Salter EG. Anatomy and potential clinical significance of the vastoadductor membrane. *Surg Radiol Anat* 2007; 29: 569-73.
3. Elazab EE. Morphological study and relations of the fascia vasto-adductoria. *Surg Radiol Anat* 2017; 39: 1085-95.
4. Bendtsen TF, Moriggl B, Chan V, Børglum J. Basic topography of the saphenous nerve in the femoral triangle and the adductor canal. *Reg Anesth Pain Med* 2015; 40: 391-2.
5. Chin KJ, Versyck B, Elsharkawy H, Rojas Gomez MF, Sala-Blanch X, Reina MA. Anatomical basis of fascial plane blocks. *Reg Anesth Pain Med* 2021; 46: 581-99.
6. Lee B, Park SJ, Park KK, Kim HJ, Lee YS, Choi YS. Optimal location for continuous catheter analgesia among the femoral triangle, proximal, or distal adductor canal after total knee arthroplasty: a randomized double-blind controlled trial. *Reg Anesth Pain Med* 2022; 47: 353-8.
7. Vora MU, Nicholas TA, Kassel CA, Grant SA. Adductor canal block for knee surgical procedures: review article. *J Clin Anesth* 2016; 35: 295-303.
8. Jæger P, Jenstrup MT, Lund J, Siersma V, Brøndum V, Hilsted KL, et al. Optimal volume of local anaesthetic for adductor canal block: using the continual reassessment method to estimate ED95. *Br J Anaesth* 2015; 115: 920-6.
9. Bendtsen TF, Moriggl B, Chan V, Børglum J. The optimal analgesic block for total knee arthroplasty. *Reg Anesth Pain Med* 2016; 41: 711-9.
10. Runge C, Moriggl B, Børglum J, Bendtsen TF. The spread of ultrasound-guided injectate from the adductor canal to the genicular branch of the posterior obturator nerve and the popliteal plexus: a cadaveric study. *Reg Anesth Pain Med* 2017; 42: 725-30.
11. Tran J, Chan VW, Peng PW, Agur AM. Evaluation of the proximal adductor canal block injectate spread: a cadaveric study. *Reg Anesth Pain Med* 2019. Advance Access published on Dec 25, 2019. doi: 10.1136/rapm-2019-101091.
12. Tran J, Peng PW, Lam K, Baig E, Agur AM, Gofeld M. Anatomical study of the innervation of anterior knee joint capsule: implication for image-guided intervention. *Reg Anesth Pain Med* 2018; 43: 407-14.
13. Gesslbauer B, Hruba LA, Roche AD, Farina D, Blumer R, Aszmann OC. Axonal components of nerves innervating the human arm. *Ann Neurol* 2017; 82: 396-408.
14. Wong WY, Bjørn S, Strid JM, Børglum J, Bendtsen TF. Defining the location of the adductor canal using ultrasound. *Reg Anesth Pain Med* 2017; 42: 241-5.
15. Laurant D, Peng P, Girón Arango L, Niazi AU, Chan VW, Agur A, et al. The nerves of the adductor canal and the innervation of the knee: an anatomic study. *Reg Anesth Pain Med* 2016; 41: 321-7.
16. Thiranagama R. Nerve supply of the human vastus medialis muscle. *J Anat* 1990; 170: 193-8.
17. Nada E, Elmansoury A, Elkassabany N, Whitney ER. Location of the entry point of the muscular branch of the nerve to vastus medialis. *Br J Anaesth* 2021; 127: e58-60.